POAC'11
Montréal, Canada

Proceedings of the 21st International Conference on
Port and Ocean Engineering under Arctic Conditions
July 10-14, 2011
Montréal, Canada

POAC11-064

DATA FOR CRUSHING FORMULA

T. Kärnä [1], D.M. Masterson [2]

[1]Karna Research and Consulting, Helsinki, Finland

[2] Chevron Canada Limited, Calgary, Canada

ABSTRACT

This paper addresses the global ice forces on vertical offshore structures. The new design standard ISO 19906 provides a new formula for calculating level ice forces based on full-scale data from the Beaufort Sea and the Baltic Sea. The first data set concerns wide structures in arctic conditions while the second data set was obtained from a narrow structure in a temperate sea area. Based on the data analysis, the size effect is expressed in terms of the ice thickness and the aspect ratio. Conditions where the aspect ratio is in excess of 2 and the ice thickness in the range from 0.2 m to about 10 m are covered.

The data clearly shows that the ice strength depends on the sea area where the structure is deployed. Therefore, the global pressure formula employs an ice strength parameter that needs to be determined separately for each ice regime. Values are provided for the Beaufort Sea and for the Baltic Sea. In addition, the standard describes methods that can be used to extrapolate to other sea areas.

INTRODUCTION

When a floe composed of level ice is acting against a vertical offshore structure and fails by crushing, it creates a global action that is expressed as

$$F_G = p_G \cdot h \cdot w \qquad (1)$$

where p_G is the global pressure, h is the ice thickness and w is the width of the structure. According to the standard ISO 19906, the global pressure can be determined by the equation

$$p_G = C_R \left(\frac{h}{h_1} \right)^n \left(\frac{w}{h} \right)^m \qquad (2)$$

where

p_G is the global average ice pressure, expressed in megapascals;

w is the projected width of the structure, expressed in metres;

h is the thickness of the ice sheet, expressed in metres;

h_1 is a reference thickness of 1 m;

m is an empirical coefficient equal to −0.16;

n is an empirical coefficient, equal to $-0.50 + h/5$ for $h < 1{,}0$ m, and to −0.30 for $h \geq 1.0$ m;

C_R is the ice strength coefficient, expressed in megapascals.

The global pressure represents the largest peak value in a time-varying ice action and an average pressure over the nominal contact area of $A_N = h \cdot w$. The expression (2) contains a parameter for the ice strength and two exponential terms, $(h/h_1)^n$ and $(w/h)^m$, which together take account of the size effects. Equation (2) applies for rigid structures with aspect ratios w/h greater than 2, where the waterline displacement, obtained as a static response to the representative ice action, is typically less than 10 mm.

Equation (2) was derived by using full-scale data from the Beaufort Sea, the Baltic Sea and the Bohai Sea. The objective of this paper is to describe this data and to show how accurately the data can be predicted by Eq. (2).

ISO 19906 uses the term *ice action* for the external ice load applied on the structure. The term *ice force* is used herein in the same meaning.

INFLUENCE OF THE ICE THICKNESS

Equation (2) assumes that the global pressure varies with the ice thickness as $p_G \propto h^{n-m}$, where n and m are experimental parameters. Figures 1 to 5 show how this relationship can be seen in various data sets. We will simplify this relationship by using the notation $n^* = n\text{-}m$. The relationship $p \propto h^{n^*}$ then applies for any fixed value of the width, including local pressures on narrow panels that are commonly used in field tests.

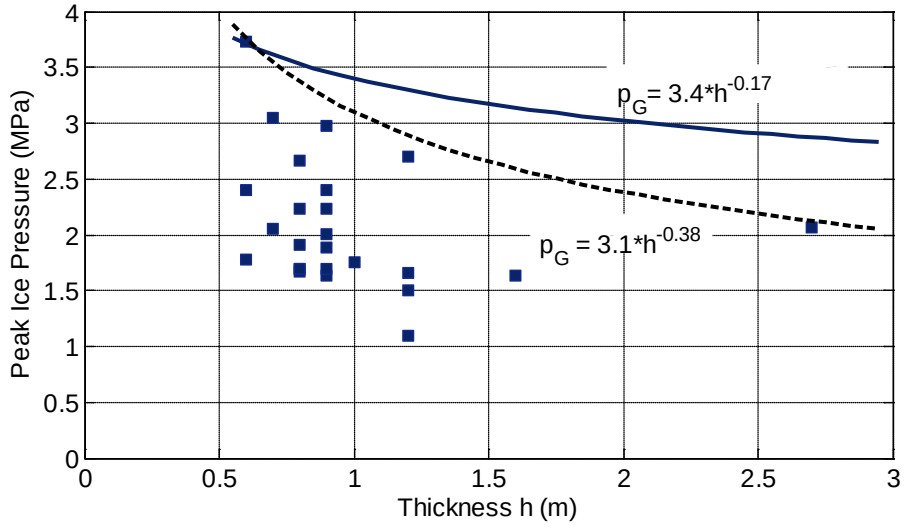

Figure 1. Maximum panel pressure as a function of ice thickness- Panel width w = 1.13 m, (Jefferies and Spencer, 1989, Table 8.2).

Figure 1 shows results of a reanalysis of data that were obtained from 25 events in 10.11.1985-12.05.1986 while the Molikpaq structure was deployed in the Amauligak I-65. This data concerns local pressures created by first-year ice on 1.13 m wide load panels. Referring to laboratory data provided by Sodhi and Morris (1984), Jefferies and Spencer assume first that the aspect ratio effect can be neglected (i.e. $m = 0$) if $w/h > 10$. Combining the Amauligak data with the laboratory data provided by Timco (1986), they then find that $n^* = n = -0.17$. This appears to be the basis for the relationship $p_G \propto h^{-0.174}$ (for $w/h > 10$ with $m = 0$) that the Canadian standard S471-4 uses for the size effect. The thickness effect represented by this relationship is supported by further data on multi-year ice forces as shown below in Fig. 3.

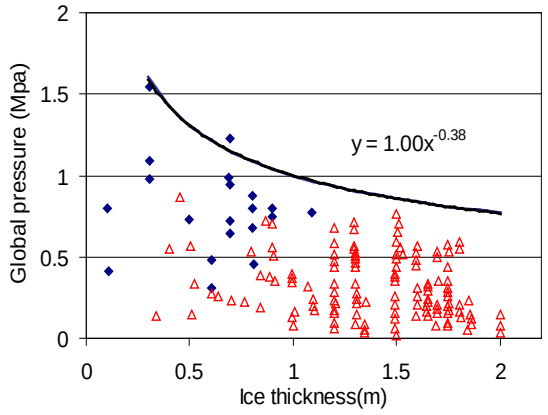

Figure 2. Global pressures due to first-year ice. Data normalized for $w = 162$ m. (Blanchet 1998, Fig. 7). Blue dots show Molikpad data.

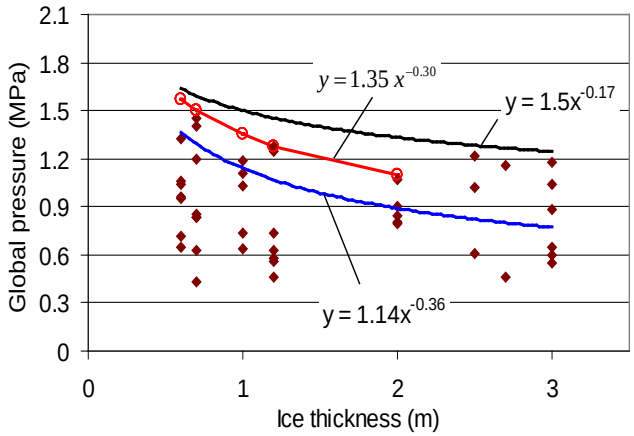

Figure 3. Peak global pressures experienced by Molikpaq in 1985/86. $w = 60$ m. (Wright 1998).

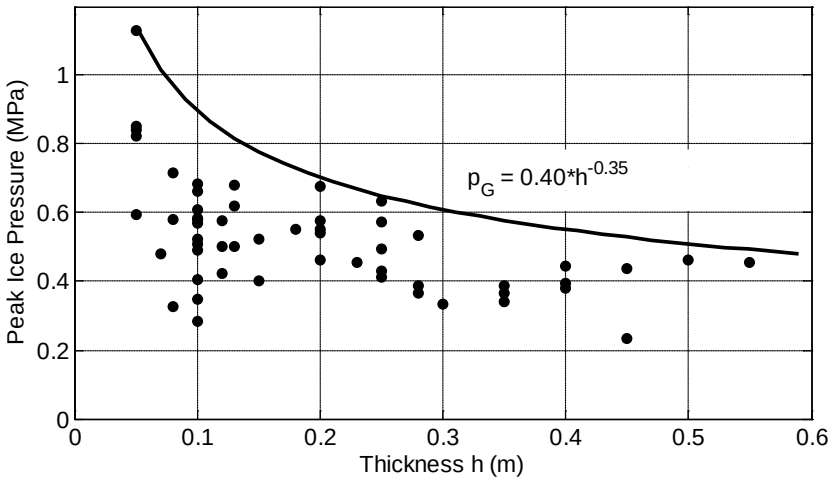

Figure 4. Global pressures measured on a 2.02 m wide leg of a jacket structure in the Bohai Sea, Wessels and Jochmann (1991). 95%-values of peak frequency distribution are shown. Ice speed varied between 0.10 m/s and 0.50 m/s.

It is of interest to notice that the data shown in Fig. 1 can be bounded also by a curve $p \propto h^{-0.38}$, which shows a stronger dependence on the ice thickness. Similar relationships can be seen in the data analysed by Blanchet (1998), Fig. 2, Wright (1998), Fig. 3 as well as Wessels and Jochmann (1991), Fig. 4. The data points shown in Fig. 2 are from a data base described by Blanchet and DeFranco (1996). This data base contains measurements that were conducted in the time frame 1966 to 1987 on bridge piers and several offshore structures, including Molikpaq.

The data shown in Fig. 3 concerns both first-year ice ($h \leq 2$ m) and multi-year ice ($h > 2$ m). The enveloping curve for first-year ice is given by $p_G = 1.35 \cdot h^{-0.30}$ (h in meters and p_G in megapascals) while the corresponding relationship for all data, including multi-year ice is $p_G = 1.5 \cdot h^{-0.17}$, which is the same as the global pressure formula in S471-04.

Figure 5 shows local pressures measured on a 7.5 m wide lighthouse in the Baltic Sea. The data points were determined from events of ice crushing by averaging the maximum peak pressure measured on five to nine different load panels. This data indicates slightly stronger dependence on the ice thickness than the data in Figs. 1 to 4. It is appreciated, however that all data points in the range of $h > 0.6$ m are due to the action of rafted ice, which is not necessarily as strong as thermally grown level ice.

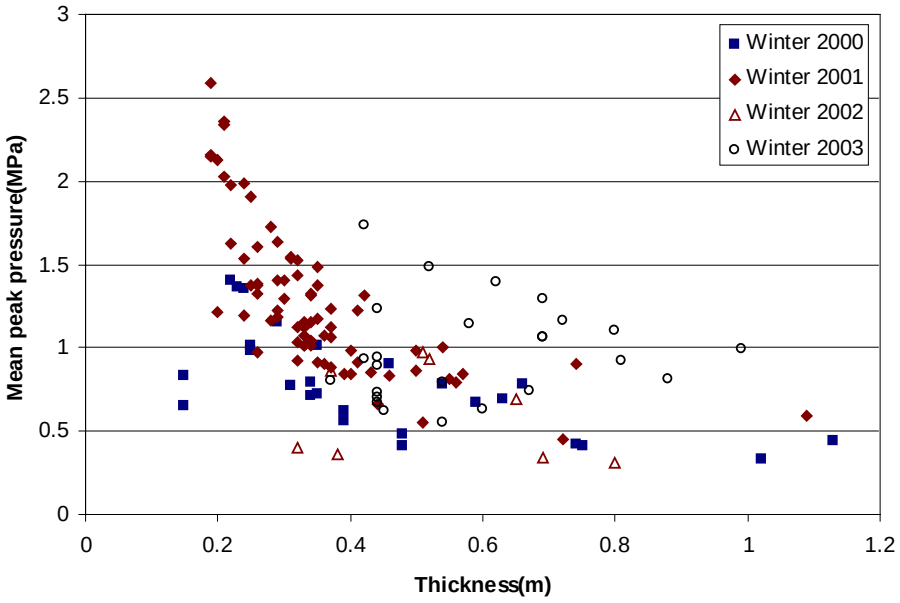

Figure 5. Maximum peak values of the panel pressures measured at the lighthouse Norströmsgrund. Data on stationary brittle crushing. Bounding curve p (Mpa) = $1.52 \cdot h^{n}$, where $n^* = -0.52$. Panel width $w = 1.2$ m. (Kärnä and Qu 2005, Fig. 17b, 18a).

As a summary, the data described above suggest that the thickness effect can be represented by the relationship $p \propto h^{n^*}$, where the exponent $n^* = n\text{-}m$ varies in the range from -0.30 to -0.40 for first-year level ice in the thickness range of $h < 1.5$ m. However, the value of the exponent is about $n^* \approx -0.17$ when both first-year ice and multi-year ice are considered.

INFLUENCE OF THE ASPECT RATIO

Data obtained in the LOLIEF/STRICE project (Schwarz and Jochmann 2001) were used to determine the exponent *m* that is used in Eq. (2) to consider the influence of the aspect ratio. Data on events with continuous crushing were used. A spectral method (Kärnä et al. 2007) was first derived to determine the global pressure by using measured local pressures as input. Figure 6 shows how this method predicts the relationship between the aspect ratio and global pressure on a flat-faced structure. This result was calculated by assuming that the maximum peak pressure on a local contact area (h = 1 m, w = 1 m) is 1 MPa. Furthermore, the coefficient of variation of the ice forces on these local contact areas was assumed as 0.40, which was typical in the data concerned. The maximum global ice pressure was determined as the mean pressure plus four times the standard deviation. Under these assumptions the mean value of the global pressure was found as 0.385 MPa for all aspect ratios.

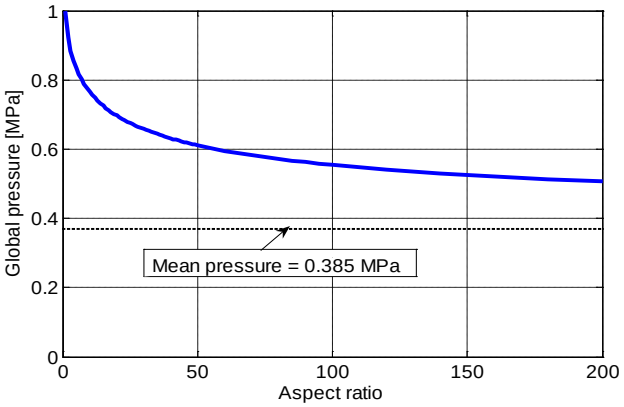

Figure 6. Global pressure as a function of the aspect ratio *w/h*.

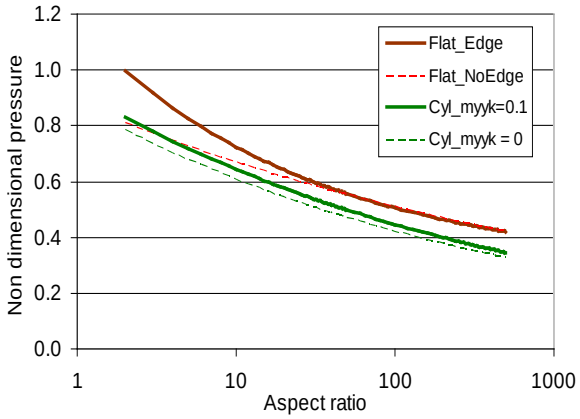

Figure 7. Comparison of the non-dimensional pressure function *f (w/h)* for flat and cylindrical structures.

The result depicted in Fig. 6 shows that the global pressure decreases with the aspect ratio towards the mean value of the global pressure. This means that the variations in a time-record of a global ice action are small if the structure is wide. For a narrow structure, however, the dynamic component in the ice action record can be significant. It is also of interest to notice that the global pressure decreases with the aspect ratio for all values of *w/h*. This feature is in contrast with some earlier results, which assume that the aspect ratio effect is insignificant in the range $w/h > 10$. Such a result has been supported by a spatial correlation analysis, which is also known as probabilistic averaging. Such a method does not consider the time-wise correlation of the local forces. Both spatial-and time-correlation are considered in the spectral method that was used for Fig. 6.

The spectral method described above was applied by Kärnä and Qu (2005) to determine the function $f\,(w/h)$ in the expression

$$p_G = p_L \; f\,(w/h) \qquad (3)$$

where p_L is the pressure on a local area that has a width of $w_L \le w$. The aspect ratio of this local area was selected as $w_L/h = 2$, which was typical for the data obtained in the STRICE project.

The function $f\,(w/h)$ was determined separately for flat and cylindrical structures for aspect ratios $w/h \geq 2$. Both compressive ice forces and tangential forces arising from kinetic friction were considered while determining the global forces on cylindrical structures. Results are shown in Fig. 7. The curve "Flat_Edge" was determined by assuming that the pressures on a flat, rectangular structure are higher close to the corners of the structure than in the central areas of the ice-structure interface. This effect was ignored in the curve "Flat_NoEdge". Notice that the shape of the functions $f\,(w/h)$ are different in Figs. 6 and 7 due to the logarithmic scale of the horizontal axis in Fig. 7.

Figure 7 shows that the global ice forces on a flat structure are slightly higher than on a cylindrical structure. The difference is, however small and can be neglected. A separate study (Kärnä and Qu, 2005) showed furthermore that the relationships obtained in Fig. 7 can be approximated as $f\,(w/h) \approx (w/h)^m$, where $m = -0.16$. This result was used in Eq. (2).

VALIDATION OF THE SIZE EFFECT

Having the exponent m of Eq. (2) determined as $m = -0.16$, we find from the thickness effects discussed above that the exponent $n = n^* - m$ should change from a value around -0.45 for very thin ice to about -0.30 for thick ice. This is achieved with the expressions that are shown for the exponent n in the clarification of Eq. (2). The size effect predicted by Eq. (2) is compared below with data obtained in the Beaufort Sea and in the Baltic Sea.

Beaufort Sea data

Figure 8 shows Molikpaq data obtained at Amauligak I-65. Only events with compressive ice failure are considered.

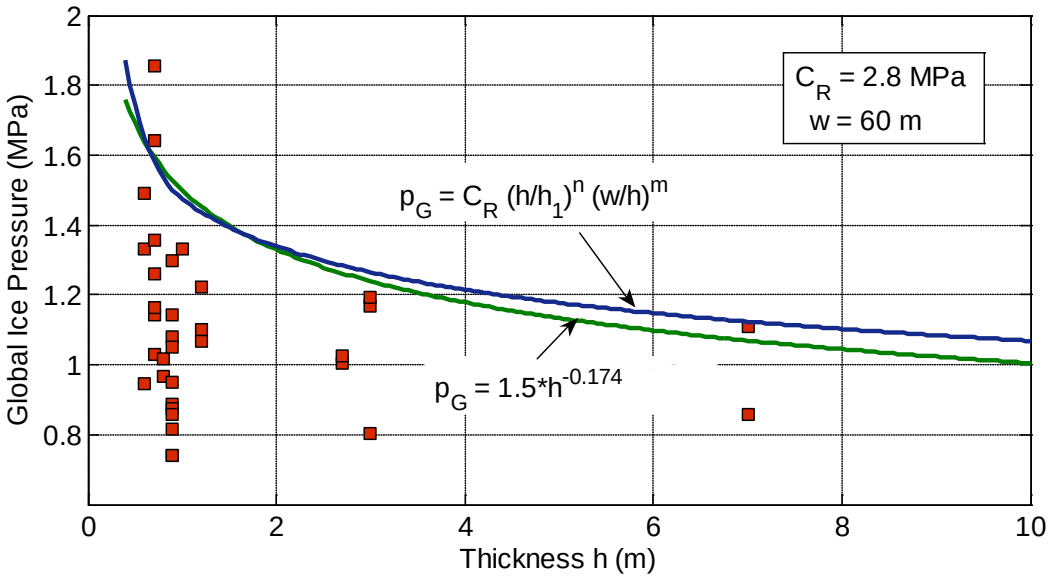

Figure 8. Comparison of measured global pressures (Timco & Johnston 2004, Table 4) and predictions by the standards ISO 19906 and S471-04.

Figure 8 also shows global pressure prediction obtained from Eq. (2) and from the function $p_G = 1.5 \cdot h^{-0.174}$ that has been used in Canadian standard S471-04 and engineering practice (Masterson and Spencer 2001). A good agreement is achieved between the two formulas if the strength parameter of Eq. (2) is selected as C_R = 2.8 MPa. Both of these expressions envelope all data points except for two points.

Baltic Sea data

Figure 9 shows directly measured values of the global pressure from ice forces on the lighthouse Norströmsgund (Kärnä and Qu 2005), which is located in the Bothnian Bay, the northernmost part of the Baltic Sea. The pressure values were obtained in winters 2000, 2001 and 2003. These data points were not used for the derivation of Eq. (2). Figure 9 shows the predicted annual maximum for the structure concerned. The predicted values were obtained from the "Baltic model" (Kärnä et al. 2006a), which was obtained from the local pressures by using the spectral model described by Kärnä et al. (2007).

It can be seen that the expected annual maxima of the global pressures that are obtained by applying the spectral model on the panel pressures are about 40% higher than the directly measured global pressures. The difference can be explained by two phenomena. First, the time exposure was much higher for events where at least some load panels were recording ice forces as compared to events where all load panels that were needed for global pressure determination were active. Second, visual observations (Kärnä and Jochmann 2003) showed that the relatively thin ice that was acting on the structure was experiencing flexural displacements during continuous crushing (mixed mode failure). This phenomenon obviously reduces the global pressure while the maximum values of the measured local pressures are unaffected.

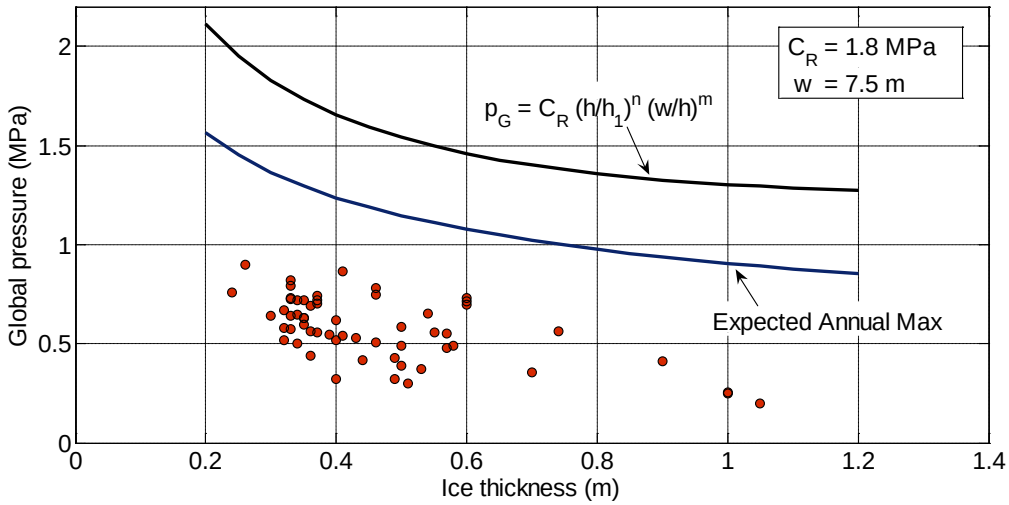

Figure 9. Comparison of measured and predicted global pressures at Norströmsgrund lighthouse.

Figure 9 also shows the function $p_G(h)$ as obtained from Eq. (2) when the ice strength parameter is selected as C_R = 1.8 MPa. The determination of the ice strength is discussed further in the next section

ICE STRENGTH

Masterson et al. (2000) recognize that ice in arctic sea areas is stronger than in sub-arctic or more temperate sea areas. They suggest that ice-infested sea areas can be divided in three zones to consider the severity of ice conditions and the influence of local climate. This approach is adopted in ISO 19906 by assuming that the ice strength parameter C_R of Eq. (2) has a different value in different ice regimes. Based on analysis of both first-year and multi-year data from the Beaufort Sea, it is suggested that $C_R = 2.8$ MPa for arctic conditions. A lower value of $C_R = 1.8$ MPa has been found to be appropriate for temperate sea areas, such as the northern part of the Baltic Sea where only first-year ice can be met. The ice is also warmer in temperate ice regimes than in arctic seas, further justifying a lower value of C_R.

The data points shown in Fig. 8 have been obtained from events where the far-field speed of the ice floes acting on the Molikpaq structure varied between 0.01 m/s and 0.42 m/s. Data analysis by Jefferies et al. (2008) suggest that global pressures experienced by Molikpaq may have increased up to 25% at an ice speed where the ice failure mode changes from simultaneous crushing or phase lock to intermittent crushing. It can be inferred from laboratory data (Sodhi, 2001, Fig. 11) that this kind of magnification of the external ice load may occur for compliant structures at a transitional ice speed where the ice failure mode changes from brittle to ductile ice failure.

Therefore, the data that was used to obtain the ice strength value of $C_R = 2.8$ MPa for arctic conditions contains effects of ice speed and the compliance of the structure. This is not the case for the STRICE data that was used for the strength value of $C_R = 1.8$ MPa for the Bothnian Bay. Effects of ice speed and structure compliance are not incorporated in that part of STRICE data that was used here. Due to this reason, the value $C_R = 1.8$ MPa was derived by applying a multiplying factor of 1.4 on the values that yield global pressures at the level of expected annual maximum (see Fig. 9).

This increase in the ice strength parameter is considered sufficient to cover the influence of the ice speed and structure compliance when the model based on STRICE data is used for more flexible structures. An increase in the ice strength parameter was needed also to consider a second kind of magnification effect. The time-varying component of the ice force can be significant in narrow structures. In such conditions the inertia forces create a dynamic magnification in internal stresses as compared to stresses that are obtained by static calculation from the peak values of the external force.

All field data that were used to derive Eq. (2) have been obtained in measurement projects that have lasted only a short period, from one to five winters. It can be considered, therefore that the values that were determined for the ice strength parameter C_R correspond to a return period of one year to about three years. The amount and quality of the data that were obtained in the STRICE project was sufficient for an extreme value analysis of both local and global pressures. Based on such an analysis, Figure 10 shows how the ice strength parameter varies with the return period (Kärnä and Qu, 2005; Kärnä 2006b).

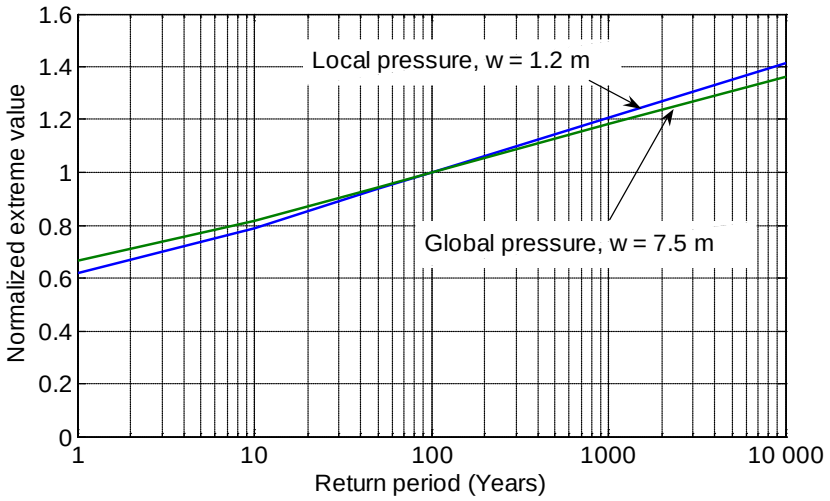

Figure 10. Extreme values of global and local pressures as function of the return period. The extreme values are normalized by the 100-year value.

DISCUSSION

Restriction on the aspect ratio

Equation (2) applies for conditions where the aspect ratio is in the range of $w/h > 2$. Figure 11 shows a data point for $w/h = 2$. The lighthouse Björnlack failed in winter 1985 due to heavy ice forces. Based on a detailed analysis, Engelbrekson (1987) conclude that the global pressure at failure was 2.6 MPa.

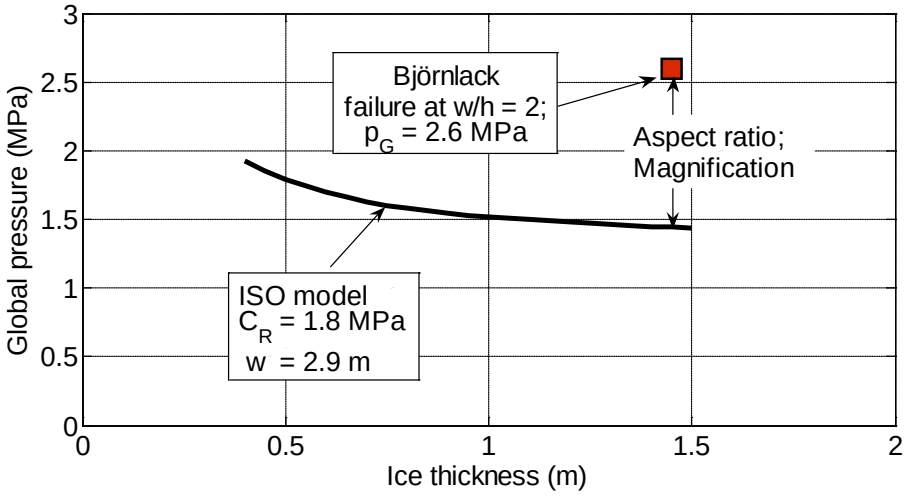

Figure 11. Predicted global pressure and pressure at failure in the lighthouse Björnlack, 1985.

Figure 11 shows that the characteristic value of the global pressure that is obtained from Eq. (2) significantly underestimates the real ice pressure. It is obvious, therefore that the aspect ratio

effect incorporated in Eq. (2) is not sufficiently strong for small aspect ratios. This problem arises from the data analysis method that was used. The load panels that are measuring local pressures on a wider structure do not capture effects of a 3D confinement that arise in the ice sheet acting on a very narrow structure. Määttänen and Kärnä (2011) discuss this problem and propose a correction.

Masterson and Spencer, 2001, indicate in Figure 8 that for loaded areas less than 30 m^2 the pressure is 8.5 $A^{-0.5}$. In the above case, the loaded area is 1.4m x 2.8m or 3.9 m^2 and the predicted pressure is 4.3 MPa. However, since the Baltic is, according to Masterson et al, 2000, in Zone II, then the pressure vs. area relationship appropriate for Björnlack would be 4 $A^{-0.5}$ = 2.34 MPa. This pressure is very close to the pressure derived by Engelbrekson. This is not surprising since the pressure vs. area relationship from Masterson and Spencer considers the 3D confinement in such a situation.

A second possible reason for the discrepancy shown in Fig. 11 is that the magnification factor of 1.40 that is inherently included in the ice strength parameter value obtained from the Baltic Sea is not sufficiently high for such a narrow structure. Kärnä et al. (2006c, Fig. 5) used a spectral model to estimate the dynamic magnification in conditions where ice is acting on the structure in the mode of continuous brittle crushing. They conclude that the internal stresses obtained by a static calculation from Eqs. (1) and (2) should be multiplied by a factor of 1.4 to 2.0 if the natural frequency varies correspondingly from 4.0 Hz to 1.0 Hz. The values of the aspect ratio and damping ratio were assumed as 2.0 and 0.0 in this calculation.

A third possibility to explain the high global pressure that was inferred from the event of structure failure (Fig. 11) is that the structure has experienced an event of frequency lock-in.

Temperature effects

Schwarz and Jochmann (2009) re-analysed LOLEIF/STRICE data, paying special attention to the air temperature. A relationship between compressive strength and ice temperature was used to normalize measured panel pressures for an air temperature of -7^{o}C. The results indicate that after such a transformation, the maximum values of the ice pressure are almost independent of the ice thickness.

This approach is infeasible for the large amount of data that is needed to derive Eq. (2) for various ice regimes. It can also be argued that ice actions on structures occur at a variety of ambient temperatures, not just at -7^{o}C. This justifies the approach that was used for Eq. (2). Data on ice forces were used without any corrections for the temperature effects.

CONCLUSIONS

The standard ISO 19906 contains a new expression for the global pressures acting on vertical offshore structures. This equation was obtained from measurements that have been made on full-scale structures in the Beaufort Sea, in the Baltic Sea and in the Bohai Sea. The data concerned was described in this paper as well as the data analysis methods that were used.

REFERENCES

Blanchet, D. and DeFranco, S.J., 1996, Global first-year ice loads: Scale effect and non-simultaneous failure. Proc. IAHR Ice Symposium, Beijing, China, August 27-30, Vol. 1, pp. 203-213.

Blanchet, D. (1998). Ice loads from first-year ice ridges and rubble fields. *Can. J. Civ. Eng*., Vol. 25, pp. 206 - 219.

Engelbrektson, A. (1987). A study of the Björnlack overloading event in April 1985. Study Project Ice Forces against Offshore Structures, Report No 1. Evaluation of extreme ice forces on a lighthouse in the Bothnian Bay. VBB Project M7334, Final Report Jan. 15, 1987. 34 p.

ISO 19906:2010(E). Arctic Offshore structures. Petroleum and natural gas industries. 474 p.

Jefferies, M.H. and P.A. Spencer, P.A., 1989. Ice loading on an offshore structure. Phase 1B: Dynamic ice/structure interaction. Main Report: Volume 1 of 2, 375 p.

Jefferies, M., Kärnä, T. and Løset, S., 2008. Field data on the magnification of ice loads on vertical structures, Proc. IAHR Int. Symp. on Ice, Vancouver, 6-11 July, Vol. 2, pp. 1115-1133, 2008

Kärnä, T & Jochmann, P. 2003. Field observations on ice failure modes. Proc. 17th International Conference on Port and Ocean Engineering under Arctic Conditions (POAC'03). Trondheim, Norway, June 16-19, Vol 2, pp. 839-848.

Kärnä, T. and Qu, Y., 2005. Analysis of the size effect tin ice crushing – edition 2. VTT, Internal Report RTE50-IR-6/2005, Version 1.3, 26.08.2009, 205 p.

Kärnä, T., Qu, Y. and Yue, Q.J., 2006(a). Baltic model of global ice forces on vertical structures. Proc. 18th IAHR Symposium on Ice. Sapporo, Japan, 28-31 Aug. 2006. Vol 1, pp. 253-260.

Kärnä, T., Qu, Y. and Yue, Q.J., 2006(b). An extreme value analysis of local pressures. Proc. International Conference and Exhibition on Performance of Ships and Structures in Ice. ICETECH-06. July 16-19. Banff. Alberta, Canada.

Kärnä, T., Qu, Y. and Yue, Q.J. 2006(c). An equivalent lateral force for continuous crushing. Proc. 25th Int. Conf on Offshore Mechanics and Arctic. Eng. June 4-9, Hamburg, Germany. Paper No OMAE 2006-92648.

Kärnä, T., Qu. Y., Yue, Q.J., Bi, X.J. and Kuehnlein W. (2007). A spectral model for forces due to ice crushing. *Journal of Offshore Mechanics and Arctic Engineering. Vol. 129, May 2007, pp. 138-14.*

Masterson, D.M., Frederking, R.M. and Truskov. P.A., 2000. Ice force and pressure determination by zone. Proc. ICETECH 2000, St.Petersburg, Russia,

Masterson, D.M and Spencer, P.A. (2001). Ice force versus aspect ratio. In: Dempsey, J.P and Shen H.H. (eds.) IUTAM Symposium on Scaling Laws in Ice Mechanics and Ice Dynamics. Kluwer 2001, pp. 31 - 42.

Määttänen, M. and Kärnä, T. (2011). ISO 19906 ice crushing load design - extension for narrow structures. Proc. 21st Int. Conf. Port Ocean Eng. under Arctic Cond., July 10-14. Montreal, Canada.

Canadian Standards Association, 2004. S471-04, General requirements, design criteria, the environment, and loads, Mississauga, ON, Canada

Schwarz, J. and Jochmann, P. 2001. Ice Force Measurements within the LOLEIF-Project. Proc. 16th Int. Conf. Port Ocean Eng. under Arctic Cond. (POAC'01), Ottawa, Ontario, Canada.

Scwarz , J. and Jochmann, P. (2009). Ice forces affected by temperature and thickness of the ice. Proc. 20th INt. Conf. Port Ocean Eng. under Arctic Cond. June 9-12. Luleå, Sweden. Paper POAC09-41.

Sodhi, D.S. and Morris, C.E., 1984. Ice forces on rigid vertical, cylindrical structures. U.S. Army Cold Regions Research and Engineering Laboratory, CRREL Report 84-33.

Sodhi, D. (2001). Crushing failure during ice-structure interaction. *Engineering Fracture Mechanics*. 68(2001) 1889-1921.

Timco, G.W., 1986. Indentation and penetration of edge loaded freshwater ice sheets in brittle range. Proc. 5th Offshore Mech. Arctic Eng. Symp., OMAE, Tokyo, Japan, Vol. 4, pp. 444-452.

Timco, G. and Johnston, M. (2004). Ice loads on the caisson structures in the Canadian Beaufort Sea. *Cold Regions Science and Technology* 38 (2004) 185 - 209.

Wessels, E. and Jochmann, P., 1991. Model-full scale correlation of ice forces on a jacket platform in the Bohai Bay. Proc. 11th Conf. Port Ocean Eng. under Arctic Conditions. St. John's, Canada, September 24-28, pp. 198 - 212.

Wright, B. (1998). Insights from Molikpaq ice loading data. Validation of Low Level Ice Forces on Coastal Structures. LOLEIF Report No. 1. EU Project - Contract MAS3-CT 97-0098. June 1988, 88 p.